EURASIP Journal on Applied Signal Processing 2005:2, 153–166

Link Adaptation for Framed Multimedia Data Transmission over a DS-CDMA Communication System

Charly Poulliat
ETIS Laboratory (UMR 8051), ENSEA/University of Cergy-Pontoise/CNRS, 6 Avenue du Ponceau, 95014 Cergy-Pontoise Cedex, France
Email: poulliat@ensea.fr

Inbar Fijalkow
ETIS Laboratory (UMR 8051), ENSEA/University of Cergy-Pontoise/CNRS, 6 Avenue du Ponceau, 95014 Cergy-Pontoise Cedex, France
Email: fijalkow@ensea.fr

David Declercq
ETIS Laboratory (UMR 8051), ENSEA/University of Cergy-Pontoise/CNRS, 6 Avenue du Ponceau, 95014 Cergy-Pontoise Cedex, France
Email: declercq@ensea.fr

Received 31 July 2003; Revised 17 May 2004

In the context of frame-based multimedia wireless transmission, a link adaptation strategy is proposed, assuming that the source decoder may accept some remaining errors at the output of the channel decoder. Based on a target mean bit error rate for erroneous frames, a minimum bit-energy-to-equivalent-noise ratio is chosen. Under this constraint, a new link adaptation criterion is proposed: the maximization of the minimum user's information rate through dynamic spreading gain and power control, allowing to guarantee a transmission for each and every user. An analytical solution to this constrained optimization problem is proposed and its performance is studied in a Rayleigh-fading environment.

Keywords and phrases: resource allocation management, link adaptation, rate and power adaptation, multirate DS-CDMA.

1. INTRODUCTION

The framework of the paper is the transmission of multimedia data through a wireless multiuser communication system such as the direct-sequence code-division multiple access (DS-CDMA). The main feature of the transmitted data is that we consider a packet-mode transmission system. On one hand, the source coder and decoder are communicating with compressed data packets, and on the other hand, DS-CDMA communication systems such as the Universal Mobile Telecommunication System (UMTS) are framed-based communication systems [1, 2]. Therefore, we can assume that the source-formatted data packets containing the compressed bitstream are sent over one or several frames at the physical layer. Moreover, the source decoder can offer some advanced features, such as robust decoding and rate adaptation capability [3]. Robust source decoding can be performed using for example an embedded forward-error correction (FEC) and synchronization techniques to mitigate the effect of remaining errors after channel decoding [3]. The source decoder can also tolerate some erroneous packets; however, the bit error rate (BER) within an erroneous packet should be lower than a critical value. The rate adaptation capability [3] allows the source decoder to adapt its rate during the transmission, depending on the available rate in the wired link and/or the possible rate on the wireless link to ensure a desired quality of service (QoS). By QoS, we mean the ability to guarantee a required BER for erroneous packets (we denote this measure as the conditional BER (CBER)), while guaranteeing a minimum user's information rate as high as possible. The rate adaptation capability of the source coder permits to consider link adaptation, that is, the adaptation of the radio resources of the physical layer depending on the variations of the communication systems (fading, number of users, etc.), as conceivable for real-time applications. As we are interested in real-time applications, we will consider that there is no

possibility of retransmission, that is, the users cannot bare a long latency (such as for an automatic repeat request (ARQ)) to get the data. Note that the following proposed link adaptation strategy can be applied to delay-tolerant applications such as video broadcasting.

Most works dealing with adaptive multirate CDMA are focused on the maximization of the total throughput in a cell [4, 5, 6] (see [7] for other multiple-input multiple-output (MIMO) systems). This is achieved through joint rate and power adaptation. The rate adaptation is itself done through either multiple codes [8], multiprocessing gains [4, 5, 6], or multirate modulations [9, 10]. When dynamic spreading gain and power control are performed, maximizing the total throughput implies that some users in the cell that are subject to a large fading are prevented from transmitting whereas these who are subject to a small fading transmit at their full power [5, 6]. This induces some latency on the wireless link for the weakest users, who are not allowed to transmit during as many frame durations as they stay in a large fading environment. This may not satisfy the concerned users. In this paper, we propose a new criterion in order to optimize the power and rate: we want to optimize the minimum of the user's information rates. Our goal is to provide a minimum QoS service for all users. When achieved, each and every user transmits at any time.

To do so, we need to evaluate the performance that can be achieved by the maximization of the minimum user's information rate through joint rate and power adaptation with perfect channel side information, subject to an instantaneous minimum bit-energy-to-equivalent-noise spectral density ratio constraint and with conventional single-user matched filter detection for each user at the base station. Based on the previous comments that the communication system is framed-based, the minimum bit-energy-to-equivalent-noise spectral density ratio constraint will depend on a new frame-based performance measure that we denote by CBER. As mentioned before, we insist on the fact that no user should be prevented from transmitting within a cell. The optimization will be achieved through dynamic processing gain and power control. We assume that a set of channel codes are available for each user. We will consider an additional maximum power constraint as there exists necessarily an upper limit on the maximum transmitter power for practical systems. We will derive some upper bounds of the considered DS-CDMA system under our link adaptation strategy. As we focus on upper bounds of the system performance, all items that can limit the practical system performance, such as nature of the feedback channel, errors in the channel estimates, or rate of the adaptation, are not considered in this paper.

The rest of the paper is organized as follows. The system model, including the definition of our new performance measure, and the notations used, are described in Section 2. A general description of our link adaptation strategy is given in Section 3. Optimal solution for unlimited continuous rates and power adaptation is provided in Section 4. Some analytical expressions and bounds are also derived. Section 5 investigates the impact of limited or discrete rates on the solution set. Some simulation results will be given in Section 6 and proofs are given Appendices A, B, and C.

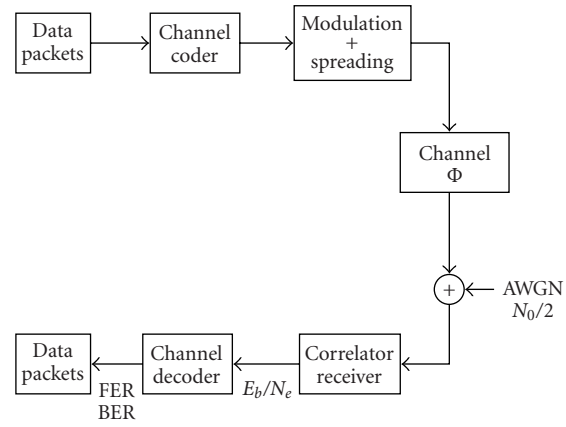

Figure 1: Communication chain.

2. SYSTEM MODEL AND NOTATIONS

2.1. Communication system description and notations

We consider the uplink transmission (i.e., from the mobiles to the base station) of a DS-CDMA communication system composed of a transmitter (convolutional channel coder and spreader) and a receiver (decorrelator + Viterbi decoder) as in Figure 1. At the base station, the receiver is the conventional single-user matched filter detector for each user. The wireless propagation channel is assumed to be a block Rayleigh-fading channel (the fading is supposed to be constant over a frame duration) and affected by an additive white Gaussian noise (AWGN). We assume that there are N_u users in the system inducing white and Gaussian interference. Let S_k and R_k be, respectively, the spreading factor and the channel coding rate associated with user k. BPSK modulation with amplitudes $\{-1, +1\}$ is used for each user. At the transmitter, the pulse shaping filter generates a rectangular pulse of a one-chip duration with unit energy. Let P_k be the transmitted power and α_k be the channel gain which is assumed known and constant during a frame for user k. We assume that the number N_u of interferers is known and constant during the frame duration. This assumption is motivated by the fact that the receiver is frame-based at the physical layer and that side information can be updated each frame. The consideration of nonconstant number of interferers is beyond the scope of this paper.

2.2. Wireless link performance measure: the equivalent E_b/N_e

As DS-CDMA systems such as UMTS [2] transmit frames of a fixed time duration which implies a fixed number of chips, the number of information bits depends on the spreading factor and on the channel coding rate. For the wireless link, we can define an equivalent signal-to-noise ratio at the output of the matched filter at the frame level that takes into account all the perturbations due to the channel.

At the receiver, the matched filter output for user k' can be written as

$$\mathbf{y}_{k'} = \mathbf{x}_{k'} + \mathbf{n}_u + \mathbf{n}, \tag{1}$$

where $\mathbf{x}_{k'}$ is the transmitted symbol vector of interest for user k', $\mathbf{n}_u$ denotes the multiuser interference for user k', and $\mathbf{n}$ is the AWGN with double-sided spectral density $N_0/2$. All quantities in (1) are vectors of components corresponding to a complete frame duration. Assuming the multiuser interference is white and Gaussian (true for large spreading factors and asynchronous users, i.e., uplink) and assuming independence between $\mathbf{n}_u$ and $\mathbf{n}$, we can explicitly write [9, 11], within each frame, the bit-energy-to-equivalent-noise spectral density ratio, E_b/N_e, at the input of the channel decoder as

$$\frac{E_b(k')}{N_e(k')} = \frac{1}{R_{k'}} \frac{P_{k'}\alpha_{k'}^2 S_{k'}}{N_0 + \beta \sum_{k \neq k'} P_k \alpha_k^2}, \tag{2}$$

where $E_b(k')$ is the mean bit energy at the receiver for user k' and $N_e(k')$ is the noise-plus-user interference variance. β is a constant depending on the choice of spreading sequences. Typically, $\beta = 2/3$ for random spreading sequences. We recall that α_k is the channel gain which is assumed constant during a frame. P_k, R_k, and S_k are, respectively, the transmitted power, the channel coding rate, and the spreading factor of user k.

The performance analysis of the physical layer of this system is also equivalent to the performance analysis of a convolutional code for an AWGN channel with mean signal-to-noise ratio E_b/N_e during a frame duration. For a convolutional code with rate R, over an AWGN channel, the frame error rate (FER) can be expressed at the output of a Viterbi decoder for a terminated trellis as [12, 13]

$$\mathrm{FER} = 1 - (1 - P_e)^{K-\nu}, \tag{3}$$

where K is the number of information bits within a frame, ν is the memory of the code, and P_e is the error event probability that can be expressed as a function of E_b/N_e, as explained in the sequel. An error event of length l and Hamming weight d is a path diverging at a particular node from the reference path (here, the all-zero codeword) and merging again after l trellis sections. P_e can be approximated using the coefficients of the weight enumerator polynomial [14] as follows:

$$P_e \simeq \sum_{d=d_{\min}}^{+\infty} a_d P_d, \tag{4}$$

where a_d is the number of error events with Hamming weight d, $d_{\min}$ is the minimum distance of the code, and

$$P_d = Q\left(\sqrt{2dR\frac{E_b}{N_e}}\right) \tag{5}$$

with $Q(\cdot)$ the Gaussian tail probability function. In the same way, the BER can be deduced from the weight enumerator polynomial [14] as

$$\mathrm{BER} \simeq \sum_{d=d_{\min}}^{+\infty} c_d P_d, \tag{6}$$

where c_d is the number of erroneous information bits for all error events of Hamming weight d. For a given convolutional code, the coefficients a_d and c_d can be calculated using standard techniques based on the generalized transfer function of the encoder state diagram [15].

Using (4) and (5), BER and FER are directly related to E_b/N_e. We will thus consider E_b/N_e as our performance measure for the output of the receiver, since it is a classical performance measure for practical systems.

2.3. On the consideration of a new performance measure: the conditional bit error rate

2.3.1. Performance measure

In this section, we will present a new performance measure that can be useful to determine a suitable behavior of the system. We try to show that this measure is an alternative measure choice to the traditionally used BER or FER.

For the considered communication system, as we are interested in the performance at the output of the channel decoder, the system performance is usually described with measures such as the BER or the FER. If we now consider the source decoder side, the processing of the received data is often frame-based [3]. Moreover, a robust source decoding can be performed using for example an embedded FEC and some synchronization techniques to mitigate the effect of remaining errors after channel decoding [3]. Combining these two aspects (robust decoding and frame-based processing), we can see that we have to determine the BER at the frame level to reach the best suitable behavior for our specific source decoder, since the concealment capabilities are directly related to the remaining errors after channel decoding. It also appears to us that both measures, BER and FER, are not suitable in the case where a packet transmission mode is used and when errors in the packets are tolerated. In fact, the BER only deals with average bit error probability and does not take into account the error's correlation or burst phenomena. Thus, the BER for an erroneous frame is higher than the average BER and thus, using only BER can conduct to an unsatisfying behavior. The FER is related to the frame level, but does not benefit from the error concealment capabilities of the source decoder that can mitigate some remaining errors and thus tolerate a given BER for an erroneous frame.

Therefore, we suggest to consider, as alternative measure of performance, the CBER, which is the average BER conditional to the fact that a frame is erroneous. The CBER allows to take into account errors at the frame level and can be useful to choose the transmission parameters more suitably according to the error concealment capabilities of the source decoder.

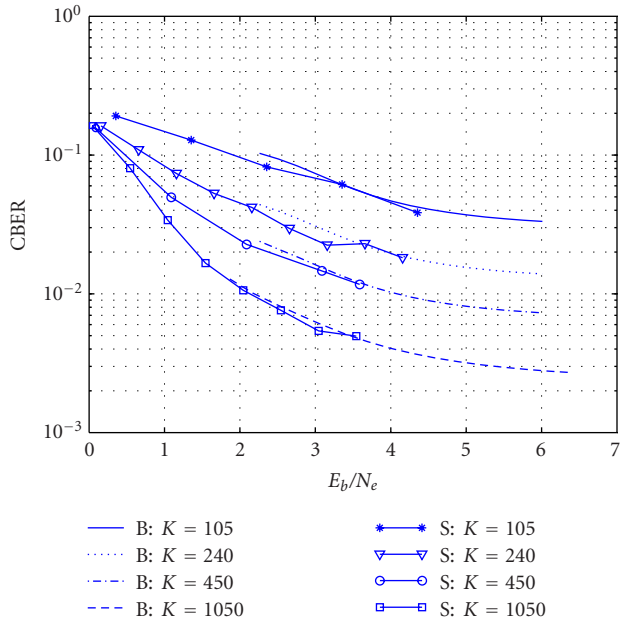

Figure 2: CBER for an AWGN channel with different frame lengths K; where (B) denotes bounds for high signal-to-noise ratios and (S) denotes simulations.

2.3.2. Definition

We define the CBER as the average BER conditional to an erroneous frame. From Bayes rule, it can be defined as the ratio between the BER and the FER:

$$\text{CBER} = \frac{\text{BER}}{\text{FER}}. \tag{7}$$

The CBER allows to take into account some correlation of errors, if no interleaving between frames is used after channel decoding. It is a good performance measure if we want to take into account that the source decoder may accept erroneous frames.

2.3.3. Bounds and simulations

The classical approximations (4) and (6) on decoding error performance are very accurate for high signal-to-noise ratios. Therefore, we can use (4) and (6) in the definition of the CBER (7) to have a good approximation of the CBER for high signal-to-noise ratios. Figure 2 shows the CBER versus the E_b/N_e for different frame lengths for the rate 1/2 convolutional code with polynomial representation in octal (561,753), as used in the UMTS standard [2]. Both bound and simulation show that above a given threshold in E_b/N_e, the CBER is constant for all frame lengths K. This can be interpreted by the fact that, for high E_b/N_e, the most probable error events are those with minimum Hamming distance $d_{\min}$. When a frame is erroneous, there is just one error event and the mean error probability is related to the average number of erroneous bits introduced by this error event. So, working in the E_b/N_e range of constant CBER provides minimum CBER for a given frame length. This property will be used in the sequel to determine the minimum E_b/N_e required to achieve the desired QoS.

3. MAXIMIZATION OF THE MINIMUM INFORMATION RATE: PROBLEM STATEMENT AND CONSTRAINTS DEFINITION

In this section, we present the constrained maximization problem induced by our goal to allow each and every user to be able to transmit at any time. As we allow each and every user to transmit during each frame duration, a link adaptation strategy based on the usual maximization of the total throughput using dynamic spreading gain and power control (see [5, 6]) is not well suited, because, as a result of the optimization problem, some users are prevented from transmitting during some frames. This is a solution we want to avoid. Therefore, in order to guarantee a minimum QoS for each user, we propose a link adaptation strategy based on the maximization of the minimum information rate with a constraint on a minimum target signal-to-equivalent-noise ratio $(E_b/N_e)_t$. The QoS issue is also to provide a minimum information rate for each user for a given required performance at the output of the channel decoder.

3.1. Information rate expression

The information rate for user k' is defined as

$$r_{k'} = \frac{R_{k'}}{S_{k'}}. \tag{8}$$

Considering (2), it becomes

$$r_{k'} = \left(\frac{E_b(k')}{N_e(k')}\right)^{-1} \frac{P_{k'}\alpha_{k'}^2}{N_0 + \beta \sum_{k \neq k'} P_k \alpha_k^2}. \tag{9}$$

Assuming that the fading gains are known and constant during a frame duration, we can see in (9) that $r_{k'}$ is a function of the communication system constants $(\{\alpha_k^2,\ k = 1,\ldots,N_u\}, N_0, \beta)$, of users' transmitted powers $\{P_k,\ k = 1,\ldots,N_u\}$, and of the $E_b(k')/N_e(k')$. $E_b(k')/N_e(k')$ is the parameter related to the QoS constraint. As explained above, we suggest to maximize the minimum rate over all users.

3.2. Optimization problem constraints

We will give here the constraints for our link adaptation optimization problem. We assume that each and every user is transmitting during a frame, so preventing a user from transmitting is not permitted, and that no retransmission is allowed. The following two constraints are considered simultaneously.

(C_1) We want to guarantee a given QoS for each user. This implies a target value for the signal-to-equivalent-noise ratio of each user. Assuming that all users belong to a same priority class, the target signal-to-equivalent-noise ratio is the same for each user. This threshold value, denoted by $(E_b/N_e)_t$, is related to the CBER constraints as explained in Section 2. According to the observations made in the previous section,

we consider the signal-to-equivalent noise range values for which the CBER is almost constant, ensuring for each frame length a "quasi-" minimal CBER. This can be formulated as follows:

$$(C_1): \frac{E_b(k)}{N_e(k)} = \left(\frac{E_b}{N_e}\right)_t, \quad k = 1,\ldots,N_u. \tag{10}$$

(C_2) Due to hardware limitation, cost constraints, or health safety, the transmitter peak power is limited to a maximum value $P_{\max}$ for the uplink transmission. The $P_{\max}$ value is assumed to be the same for all users (i.e., all mobiles are of the same type). This can be formulated as follows:

$$(C_2): 0 < P_k \leq P_{\max}, \quad k = 1,\ldots,N_u. \tag{11}$$

3.3. Optimization formulation

Our goal is to adapt the spreading gains and powers to achieve the maximization of the minimum rate. Considering (9), the maximum information rate that meets the $(E_b/N_e)_t$ (constraint (C_1)) is given, for user k', by

$$r_{k'} = \left(\frac{E_b}{N_e}\right)_t^{-1} \frac{P_{k'}\alpha_{k'}^2}{N_0 + \beta\sum_{k\neq k'} P_k\alpha_k^2}. \tag{12}$$

Thus, the maximization of the minimum information rate, under the constraints described in Section 3.2, can be expressed using (12) as follows:

$$\max_{\{P_{k'}\}} \min_{k'} r_{k'} \text{ constrained to } (C_1),\ (C_2). \tag{13}$$

Note that according to the cost function (13), the joint rate and power adaptation is reduced to a power optimization problem. The choice of information rates results from the power adaptation.

3.4. Different constraints on the rate solution sets

Solving the above optimization problem requires an optimization on the transmitted power only. Let $\mathbf{P} = (P_1,\ldots,P_{N_u})$ be the vector solution to the optimization problem. Each user's information rate is calculated knowing $\mathbf{P}$ according to (12). This induces a theoretical rate solution set taking real positive values in $\mathbb{R}_+$. However, the rates r_k being defined by (8) can only take discrete values. For instance in the UMTS standard, $R_k = \{1, 1/2, 1/3\}$ and $S_f = \{2^q | q = 0, 1, \ldots, 9\}$. We should therefore study different solution sets with additional constraints on the available space where the rates can take their values, and study the impact of such constraints on the optimal performance and on the solution to cost function (13).

Next, we will consider that possible rates resulting from the optimization problem are subject to constraints. Three kinds of a rate solution set are considered in the sequel.

(S_1) Continuous rates. The information rates can take any value in $\mathbb{R}_+$. The problem is also completely separable: first the power allocation is given by solving (13) and then the rate allocation is a straightforward application of (12). This will give upper bounds on the performance of the practical system.

(S_2) Continuous rates with boundaries constraints. This constraint takes into account that the information rate is in general bounded by a minimum and a maximum available rate.

(S_3) Discrete solution set. The solutions are bounded and belong to a discrete solution set.

4. AN OPTIMAL SOLUTION FOR CONTINUOUS RATE AND POWER ALLOCATION

In this section, we consider users' information rates as continuous variables over the entire range of positive real numbers.

4.1. Motivation of the study

In the case of continuous rates, the results of the optimization problem (13) give an upper bound on the performance of a practical system. Moreover, the obtained solution can be a useful tool to compare theoretical performance of different link adaptation schemes.

4.2. Solution to the optimization problem

Under the constraints (C_1) and (C_2), the solution to the constrained optimization problem (13) is given by the following proposition (see Appendix A for a proof).

Proposition 1. *Ordering the users indices* $\{1,\ldots,N_u\}$ *in an increasing channel gain order* $(\alpha_1^2 \leq \ldots \leq \alpha_{N_u}^2)$*, the solution to the constrained optimization problem* (13) *is given by*

$$P_k\alpha_k^2 = P_{\max}\alpha_1^2, \quad k = 1,\ldots,N_u, \tag{14}$$

where α_1 *is the weakest channel gain.*

Corollary 1. *When the maximization of the minimum rate is achieved* (14)*, each and every user has the same information rate given by*

$$r_{\max-\min} = \left(\frac{E_b}{N_e}\right)_t^{-1} \frac{P_{\max}\alpha_1^2}{N_0 + \beta(N_u - 1)P_{\max}\alpha_1^2}. \tag{15}$$

4.3. Proposed link adaptation scheme in the continuous-rate case

In the light of Section 4.2, we describe here the proposed link adaptation scheme which consists in the maximization of the minimum rate, constrained by a required $(E_b/N_e)_t$ at the input of the channel decoder based on the CBER and power limitation.

We now describe the different steps of the link adaptation strategy we propose.

(i) Select the required target signal-to-equivalent-noise ratio $(E_b/N_e)_t$. This constraint is based on the CBER ensuring that CBER is minimal for each frame length.

(ii) Knowing the channel gain amplitudes α_k and the number of users N_u in the cell, select the weakest user (associated with the minimum channel gain).

(iii) Compute powers at the transmitter according to Proposition 1.

The main advantage of this scheme is the very low computational complexity to find the optimum powers and the associated rates.

4.4. Comments on the solution

The solution found in (14) underlines the necessary tradeoff between strong and weak users. From (14), the received powers have to be equal to the same constant: $P_k\alpha_k^2 = c$, for all $k = 1,\ldots,N_u$. Thus, the users fight against the near-far effect at the base station. Each user generates the same interference. Note that the solution to the proposed link adaptation is similar to the existing techniques to avoid near-far effect, since all the received powers are equal (see [16] for a general description). The fact that the constant is equal to $P_{\max}\alpha_1^2$, where α_1 is the weakest channel gain, shows that the best achievable performance in this context is constrained by the weakest user due to his strong fading and the power limitation.

4.5. Analytical expressions and bounds in the continuous-rate case

The previous scheme gives the *instantaneous* solution to the optimization problem (13), that is to say, the solution for a given frame duration and given channel gains. We will now derive some analytical bounds on the *average* performance (in terms of the average information rate per user or average received bit energy per user) of the proposed scheme in order to evaluate the performance and compare with other link adaptation strategies. Average performance can be determined by averaging out over the probability distribution of the channel gains.

We assume that for each and every user, the channel gains α_k, considered as random variables, are independent and identically distributed and have a Rayleigh distribution parameterized by the parameter $\Omega = \mathrm{E}(\alpha_k^2)$.

4.5.1. Probability density function of the minimum channel gain

Each and every performance measure is related to the weakest channel gain α_1. As a classical result of order statistics [17], the minimum channel gain α_1 follows a Rayleigh distribution with parameter $\mathrm{E}(\alpha_1^2) = \Omega/N_u$ and the corresponding probability density function (pdf) is given by

$$f_{\alpha_1}(\alpha) = \frac{2N_u\alpha}{\Omega}e^{-N_u\alpha^2/\Omega}, \quad \alpha > 0. \tag{16}$$

Based on this result, we can now derive some analytical expressions regarding average performance and some bounds.

4.5.2. Average information rate

Using the instantaneous solution to the optimization problem for each frame (15), we can average out over the channel gains described by their pdf (16). By defining $C = (E_b/N_e)_t^{-1}P_{\max}$ and $\lambda = \beta(N_u - 1)P_{\max}$, the average information rate is given by

$$\begin{aligned}\overline{r} &= \mathrm{E}(r) = \int_0^{+\infty} r_{\max-\min} f_{\alpha_1}(\alpha)d\alpha \\ &= C\frac{N_u}{\Omega\lambda^2}e^{N_uN_0/\Omega\lambda}(I_1 - I_2)\end{aligned} \tag{17}$$

with

$$\begin{aligned}I_1 &= \frac{\Omega\lambda}{N_u}e^{-N_uN_0/\Omega\lambda}, \\ I_2 &= N_0\Gamma\left(0, \frac{N_uN_0}{\Omega\lambda}\right),\end{aligned} \tag{18}$$

where

$$\Gamma(p,z) = \int_z^{+\infty} t^{p-1}\exp(-t)dt \tag{19}$$

is the incomplete Gamma function. Note that (17) is always positive since $I_1 > I_2$. The detailed proof of (17) is given in Appendix B.

It is of practical interest (in terms of computational complexity) to derive simple bounds that can be close to exact analytical expressions for a large range of values. First, by considering (17), we can get a lower bound for $\overline{r}$ using an upper bound for I_2, which is finally given by the following expression (see the detailed proof given in Appendix C):

$$I_2 \le N_0 e^{(-N_uN_0/\Omega\lambda)}\left(\frac{N_uN_0}{\Omega\lambda}\right)^{(1/p-1)}(p-1)^{(1-2/p)}p^{(1/p-1)}, \quad \forall p > 1. \tag{20}$$

Since (20) is true for all $p > 1$, the closest upper bound is reached by optimizing the parameter p to minimize the second member of (20): for a given number of users N_u and a given noise power, the optimal value for the real parameter p, such as $p > 1$, is the one which minimizes the second member of (20). So the parameter p varies over the range of noise powers and for different values of N_u. Finally, reporting this expression in (17), we get a lower bound for $\overline{r}$.

Using (17), and since $I_2 \ge 0$, we have the following upper bound:

$$\begin{aligned}\overline{r} &\le C\frac{N_u}{\Omega\lambda^2}e^{N_uN_0/\Omega\lambda}I_1 \\ &\le \frac{C}{\lambda}\end{aligned} \tag{21}$$

and finally, we get

$$\overline{r} \le \frac{(E_b/N_e)_t^{-1}}{\beta(N_u - 1)}. \tag{22}$$

The asymptotic value of $\overline{r}$ when the noise power goes to zero cannot increase to infinity, since it is upperbounded by the multiple-access load capacity (22). The accuracy of these bounds is shown in Section 6.

4.5.3. Average bit energy

We focus on the received average bit energy. During a frame duration, the energy bit for a user is given by

$$E_b = \left(\frac{E_b}{N_e}\right)_t (N_0 + \lambda\alpha_1^2). \tag{23}$$

Then, averaging out over the pdf of the channel gains, the average bit energy per user is given by

$$\begin{aligned}\overline{E}_b &= \mathrm{E}(E_b) = \left(\frac{E_b}{N_e}\right)_t \left(N_0 + \lambda \int_0^{+\infty} \alpha^2 f_{\alpha_1}(\alpha) d\alpha\right) \\ &= \left(\frac{E_b}{N_e}\right)_t \left(N_0 + \frac{\lambda\Omega}{N_u}\right).\end{aligned} \tag{24}$$

Therefore, the average bit energy is a constant when N_0 goes to zero (low noise power). This constant is equal to $(E_b/N_e)_t(\beta(N_u - 1)P_{\max}\Omega/N_u)$. Thus, when N_u increases, the average bit energy increases due to the load of the cell. This can be interpreted as follows: at low noise power, we only have multiuser interference, which increases when N_u increases. We then have to transmit more energy per bit to fight against the multiuser interference.

We can also deduce the average signal-to-noise ratio at the input of the receiver, given by

$$\frac{\overline{E}_b}{N_0} = \left(\frac{E_b}{N_e}\right)_t \left(1 + \frac{\beta(N_u - 1)P_{\max}\Omega}{N_u N_0}\right). \tag{25}$$

In Section 6, we will compare these bounds to the simulated values to check for their validity in terms of number of users, noise power, and so forth.

5. IMPACT OF THE CONSTRAINTS ON THE RATE SOLUTION SET

In Section 3.4, we have seen that the information rates resulting from the optimization problem (13) are subject to two additional constraints for practical systems: firstly, the rates are bounded by some maximum and minimum values, and secondly, they take their values in a discrete space. Even if the continuous case can give an upper bound for practical systems, it is necessary to study the solution to the optimization problem (13) subject to the additional hypothesis (S_2) or (S_3) defined in Section 3.4. The solutions to the optimization problem with constraints (S_2) and/or (S_3) are not obvious and cannot be directly inferred from the continuous-rate case. Nevertheless, the impact of hypotheses (S_2) and (S_3) on the rate solution set can be studied by considering the following approach. We consider the rates resulting from the optimization problem (13) and we apply to these rates the hypothesis (S_2) or (S_3). This is equivalent to considering in the first case (S_2) a saturation of $r_{\max-\min}$ at the boundaries and in the second case (S_3) a quantization of $r_{\max-\min}$ values. In doing so, we will measure the performance loss on the link adaptation scheme induced by the constraints (S_2) and (S_3). We will focus on the average information rate as a measure of performance to study impact of the constraints (S_2) and (S_3) on the rate solution set.

5.1. Bounded continuous rates

In this subsection, we will consider the case of bounded continuous rates.

5.1.1. Link adaptation strategy for bounded continuous rates

Considering that the optimal rate solution to the optimization problem (13), in the continuous-rate case, given by (15), is subject to the constraint

$$r_m \le r_{\max-\min} \le r_M, \tag{26}$$

we propose a suboptimal link adaptation strategy based on the saturation of rate outside the boundaries. The different steps of the link adaptation strategy proposed in Section 4.3 for the continuous-rate case are modified as follows.

(i) Select the required target signal-to-equivalent-noise ratio $(E_b/N_e)_t$.

(ii) Knowing the channel gain amplitudes α_k and the number of users N_u in the cell, select the weakest user (associated with the minimum channel gain).

(iii) Compute powers at the transmitter according to Proposition 1.

(iv) Compute rate $r_{\max-\min}$. If $r_{\max-\min} < r_m$ (resp., $r_{\max-\min} > r_M$), then saturate $r_{\max-\min}$ to r_m (resp., to r_M).

The additional step (iv) just controls the saturation of the rate if it is outside the boundaries.

5.1.2. Average information rate

We want to evaluate the average information rate achieved when a saturation of the continuous rate solution is used. This will allow us to compare with the unlimited-rate case and to evaluate the loss of performance. Before averaging, we have to explicit $r_{\max-\min}$ with regard to the range values of the weakest channel gain α_1. Thus, considering (26), $r_{\max-\min}$ is given as follows:

$$r_{\max-\min} = \begin{cases} r_m, & \alpha_1 \le \alpha_{\min}, \\ \left(\dfrac{E_b}{N_e}\right)_t^{-1} \dfrac{P_{\max}\alpha_1^2}{N_0 + \beta(N_u - 1)P_{\max}\alpha_1^2}, & \alpha_{\min} \le \alpha_1 \le \alpha_{\max}, \\ r_M, & \alpha_{\max} \le \alpha_1, \end{cases} \tag{27}$$

where α_1 is the weakest channel gain. $\alpha_{\min}$ and $\alpha_{\max}$ are solutions to $r_{\max-\min} = r_m$ and $r_{\max-\min} = r_M$, respectively. Averaging out over the channel gains and taking into account the saturation, the average information rate is given by

$$\begin{aligned}\overline{r} &= \int_0^{+\infty} r_{\max-\min} f_{\alpha_1}(\alpha) d\alpha \\ &= \int_0^{\alpha_{\min}} r_m f_{\alpha_1}(\alpha) d\alpha + \int_{\alpha_{\min}}^{\alpha_{\max}} r_{\max-\min} f_{\alpha_1}(\alpha) d\alpha \\ &\quad + \int_{\alpha_{\max}}^{+\infty} r_M f_{\alpha_1}(\alpha) d\alpha \\ &= r_m I_m + I_P + r_M I_M,\end{aligned} \tag{28}$$

where I_m, I_M, and I_P are given by

$$\begin{aligned} I_m &= \int_0^{\alpha_{\min}} f_{\alpha_1}(\alpha)d\alpha \\ &= \int_0^{\alpha_{\min}} \frac{2N_u\alpha}{\Omega} e^{-N_u\alpha^2/\Omega} d\alpha \\ &= 1 - e^{-N_u\alpha_{\min}^2/\Omega}, \\ I_M &= 1 - \int_0^{\alpha_{\max}} f_{\alpha_1}(\alpha)d\alpha = e^{-N_u\alpha_{\max}^2/\Omega}, \\ I_P &= \int_{\alpha_{\min}}^{\alpha_{\max}} r_{\max-\min} f_{\alpha_1}(\alpha)d\alpha \\ &= \int_{\alpha_{\min}}^{\alpha_{\max}} \frac{C\alpha^2}{N_0+\lambda\alpha^2} f_{\alpha_1}(\alpha)d\alpha, \end{aligned} \tag{29}$$

where C and λ are constants previously defined in Section 4.5.2.

We focus on the calculation of I_P. Applying the same calculation techniques as in Section 4.5.2, we have

$$\begin{aligned} I_P &= \int_{\alpha_{\min}}^{\alpha_{\max}} r_{\max-\min} f_{\alpha_1}(\alpha)d\alpha \\ &= \int_{\alpha_{\min}}^{\alpha_{\max}} \frac{C\alpha^2}{N_0+\lambda\alpha^2} f_{\alpha_1}(\alpha)d\alpha \\ &= C\frac{N_u}{\Omega\lambda^2} e^{N_uN_0/\Omega\lambda} \int_{u_{\min}}^{u_{\max}} \frac{u-N_0}{u} e^{-N_uu/\Omega\lambda} du \\ &= C\frac{N_u}{\Omega\lambda^2} e^{N_uN_0/\Omega\lambda}(I_1' - I_2'), \end{aligned} \tag{30}$$

where

$$\begin{aligned} u_{\min} &= N_0 + \lambda\alpha_{\min}^2, \\ u_{\max} &= N_0 + \lambda\alpha_{\max}^2, \\ I_1' &= \frac{\Omega\lambda}{N_u}\left(e^{-N_uu_{\min}/\Omega\lambda} - e^{-N_uu_{\max}/\Omega\lambda}\right), \\ I_2' &= N_0(\Gamma(0,\nu_{\min}) - \Gamma(0,\nu_{\max})), \end{aligned} \tag{31}$$

with $\nu_{\min} = N_uu_{\min}/\Omega\lambda$ and $\nu_{\max} = N_uu_{\max}/\Omega\lambda$. $\Gamma(p,z)$ is the incomplete Gamma function given by (19).

Thus, considering (28), we can predict the asymptotic behavior of the average rate under bounded-rates constraint. For low noise powers, the average information rate converges to the maximum rate r_M. For high noise powers, the average information rate converges to the minimum rate r_m.

5.2. Finite-discrete-rate set case

In this section, we will consider the case where the rates take their values in a finite size and a discrete space. The rates r_k resulting from the optimization problem (13) must be a ratio of the available channel coding rates R_k and the available spreading factors S_k for the user k. Therefore, $r_k = R_k/S_k$ should take a finite number of discrete values. The set of available channel coding rates and spreading factors may vary from a user to another. The present constraint can be viewed as a refinement of the previous case: the rates are effectively bounded due to the discrete nature of the set, and inside the boundaries, the rates take a finite number of discrete values.

Following the approach of the preceding section, we will express analytically the performance loss induced by the finite-discrete rates constraint on the continuous rates solution set given by (15). Note that with a finite number of discrete rates, the optimization might be solved by an exhaustive search. This issue is not addressed in this paper.

After giving the modified and suboptimal link adaptation strategy we propose, we discuss the average information rate that can be reached with constraint (S_3) compared to case (S_2).

5.2.1. Modified link adaptation scheme in the finite-discrete-rate set case

Considering that the optimal rate solution to optimization problem (13), in the continuous-rate case given by (15), is submitted to the constraints (C_2) and (C_3), and that $r_{\max-\min}$ takes a discrete value depending on the user's available channel coding rates an spreading factors, we propose a suboptimal link adaptation strategy based on the quantization of rates. The different steps of the link adaptation strategy proposed in Section 4.3 are modified as follows.

(i) Select the required target signal-to-equivalent-noise ratio $(E_b/N_e)_t$.

(ii) Knowing the channel gain amplitudes α_k and the number of users N_u in the cell, select the weakest user (associated with the minimum channel gain).

(iii) Compute powers at the transmitter according to Proposition 1.

(iv) Compute rate $r_{\max-\min}$. Knowing the set of available R_k and S_k for user k, select the best suited set $\{R_k, S_k\}$ such as

$$r_k = \frac{R_k}{S_k} \le r_{\max-\min}. \tag{32}$$

The additional step (iv) controls the saturation of the rate and allows to find the best tradeoff between channel coding rate and spreading factor for the quantization.

5.2.2. Asymptotic behavior

In this section, we do not derive analytical expressions, but discuss the behavior of the proposed link adaptation strategy in the discrete case. Comparisons with the previous cases will be done in Section 6.

Similarly to the previous bounded-rate case, we can explicit the average performance in terms of average information rate. Considering a finite set of available rates $(r_k,\ k = 0,\dots,M)$, where r_0 and r_M are, respectively, the minimum and the maximum information rates available, the quantization of the optimal solution yields to the following expression for $r_{\max-\min}$:

$$r_{\max-\min} = \begin{cases} r_m, & \alpha_1 \le \alpha_0, \\ r_k, & \alpha_k \le \alpha_1 \le \alpha_{k+1},\ \forall k = 0,\dots,M-1, \\ r_M, & \alpha_M \le \alpha_1, \end{cases} \tag{33}$$

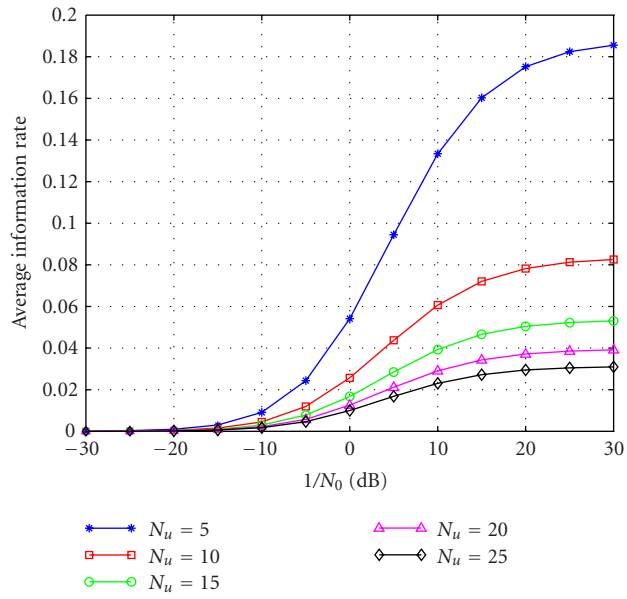

FIGURE 3: Average information rate $\overline{r}$ versus inverse noise power $1/N_0$: simulation results for $N_u = 5, 10, 15, 20, 25$.

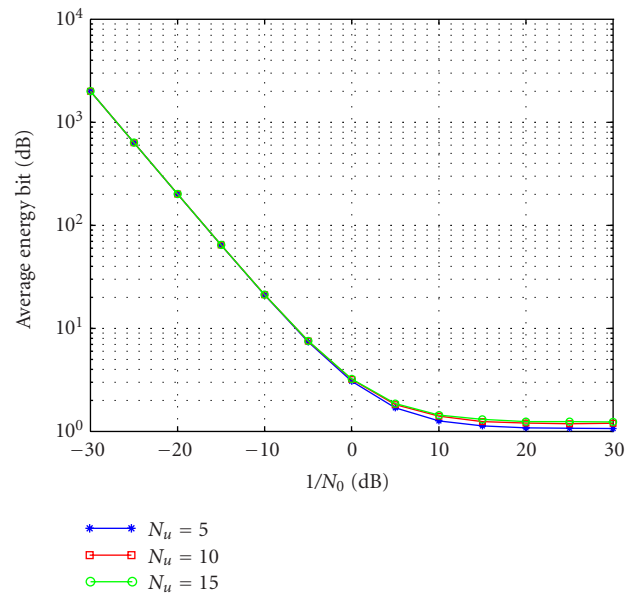

FIGURE 4: Average bit energy $\overline{E}_b$ versus inverse noise power $1/N_0$ in the continuous-rate case: simulation results for $N_u = 5, 10, 15$.

where α_k are the solutions of $r_{\max-\min}(\alpha_k) = r_k$ using (15). Averaging out over the channel gains and taking into account the quantization, the average information rate is given by

$$\begin{aligned}\overline{r} &= \int_0^{+\infty} r_{\max-\min} f_{\alpha_1}(\alpha)d\alpha \\ &= \int_0^{\alpha_0} r_0 f_{\alpha_1}(\alpha)d\alpha + \sum_{k=0}^{M-1}\int_{\alpha_k}^{\alpha_{k+1}} r_k f_{\alpha_1}(\alpha)d\alpha \\ &\quad + \int_{\alpha_M}^{+\infty} r_M f_{\alpha_1}(\alpha)d\alpha \\ &= r_0 I_0 + \sum_{k=0}^{M-1} r_k I_k + r_M I_M\end{aligned} \tag{34}$$

with

$$\begin{aligned}I_0 &= 1 - e^{-N_u\alpha_0^2/\Omega}, \\ I_M &= e^{-N_u\alpha_M^2/\Omega}, \\ I_k &= e^{-N_u\alpha_k^2/\Omega} - e^{-N_u\alpha_{k+1}^2/\Omega}.\end{aligned} \tag{35}$$

The main modification in the discrete case is that the rates below the maximum rate and above the minimum rate are quantized to discrete values. So the bounded-continuous case is an upper bound of the discrete case. Moreover, we can claim that the behavior at the boundaries are the same in both cases, that is, the rates go to the minimum rate for high noise powers and go to the maximum for low noise powers. For medium noise powers, the performance of the discrete case is upper bounded by the bounded-continuous case. How close are the performance in both cases will be discussed with simulation results in Section 6.

6. SIMULATION RESULTS

In this section, we present some simulation results in order to check for the validity of the analytical expressions and bounds we developed, and to compare the different solutions constrained by (S_1), (S_2), and (S_3). For all simulations, the users' channel gains have the same Rayleigh distribution parameterized by the parameter $\mathrm{E}(\alpha_k^2) = 1$, for all $k = 1, \ldots, N_u$. The maximum peak power is set to 1. We suppose that each and every user has only one channel coding rate R available. We set $R = 1/2$. The target signal-to-equivalent-noise ratio is set to $(E_b/N_e)_t = 3$ dB. Considering randomly chosen spreading sequences, β is equal to 2/3. Each and every user has the same available spreading factors, such that $S_f = \{2^q \mid q = 0, 1, \ldots, 9\}$. Thus, S_f is always less than or equal to 512.

First, we consider the continuous-rate case and analyze the influence of the different system parameters such as the number of users in the cell and the noise power. Analytical expressions and bounds in the continuous case are compared to the simulation results to check for their validity. Then, we study the loss of performance due to saturation and quantization rate of the solution.

6.1. Average performance for the continuous-rate case

Figures 3 and 4 give simulation results for the average information rate per user and the average bit energy versus the inverse noise power for different number of users N_u. In Figure 3, as expected, for a given noise power, the average rate decreases when the number of users N_u increases. This is due to the increase of multiuser interference when N_u increases. All curves are strictly increasing functions of the inverse of the noise power, that is, when the noise power decreases, the average rate increases. Since rates are continuous, they go to

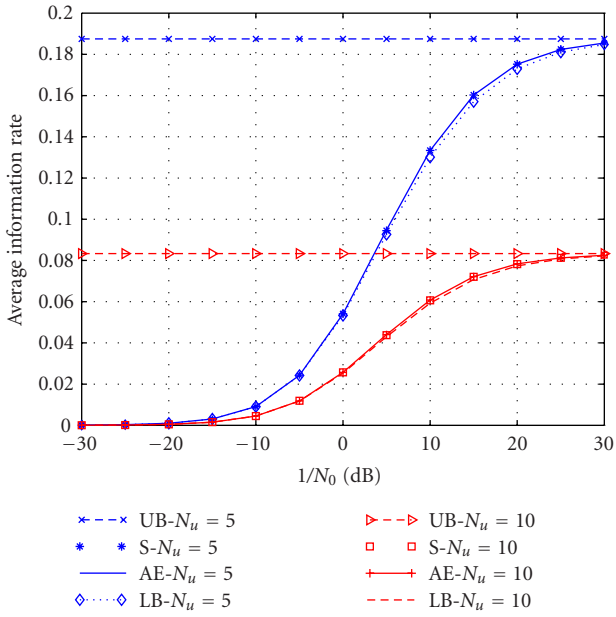

Figure 5: Average information rate $\overline{r}$ versus inverse noise power $1/N_0$ in the continuous-rate case, where (UB) denotes asymptotic upper bound, (S) simulation, (AE) analytic expression, and (LB) lower bound. $N_u = 5, 10$.

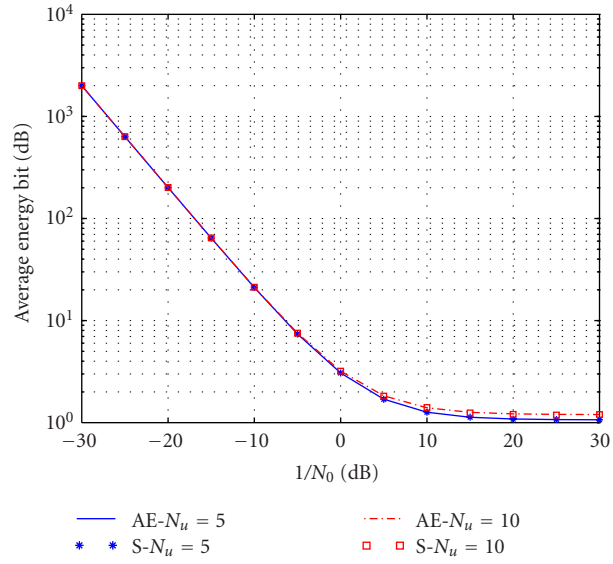

Figure 6: Average bit energy $\overline{E}_b$ versus inverse noise power $1/N_0$ in the continuous-rate case, where (AE) denotes analytic expression and (S) denotes simulation. $N_u = 5, 10$.

zero for high noise power. For low noise powers, the rates converge asymptotically to the constant given by (22). This constant is related to the maximum reachable information rate when the users are only subject to multiuser interference. As we can see, this constant is directly related to the number of users N_u. For example, when $N_u = 20$, the asymptotic value given by (22) for low noise power is 0.0395, which is the asymptotic value we observe. In Figure 4, the average bit energy for a given N_u is a strictly decreasing function of the inverse of noise power: the higher the noise power is, the higher the average transmitted bit energy has to be. This is due to the fact that, for high noise powers, the information rate is low, requiring low channel coding rates and high spreading factors. Thus, the required bit energy to transmit with the given QoS increases. For a given noise power (cf. (24)), the average bit energy increases with increasing N_u. The asymptotic value for low noise power is given by (24) when N_0 goes to zero. For example for $N_u = 20$, $\overline{E}_b$ theoretically goes to 1.2444. Simulation results are close to this value for low noise powers.

Figures 5 and 6 allow to compare analytical expressions and bounds to simulation results. Figure 5 displays results for the average information rate and Figure 6 displays results for the average bit energy. In Figure 6, both analytical expressions and simulations are very close. In Figure 5, we compare for $N_u = 5$ and $N_u = 10$ the analytical expressions given by (17), and the bounds given by (22) and by (20) with simulations. The bound given by (20) is obtained by finding, for a given number of user N_u and a given noise power N_0, the value of the parameter p which minimizes the second member of (20). Thus, (22) gives the asymptotic value of reachable average information rate in presence of multiuser interference only. Equation (20), when optimized with the parameter value p for a given noise power, gives a tight lower bound over the entire range of noise power values.

6.2. Impact of rates saturation and quantization

Here, we study the influence of saturation and quantization of the solution to the continuous-rate case. First, we check for the validity of the analytical expression of the average information rate when saturation only is used. Then, we compare the different link adaptation schemes when saturation and quantization are used with the continuous-rate case.

Figure 7 shows simulation results and analytical expressions for the bounded-continuous-rate and the finite-discrete-rate cases. The analytical expressions are given by (28) and (34). The spreading factors are bounded in both cases by $S_{f\max} = 512$ and $S_{f\min} = 8$ for $N_u = 5$, and $S_{f\min} = 16$ for $N_u = 10$. We have a good matching of simulation curves with theoretical expressions. For high noise power, the minimum rate is the same and is equal to 1/1024. The rates obtained by simulation converge to this asymptotic value for high noise power. For low noise power, the asymptotic expected rates are given for $N_u = 5$ and $N_u = 10$, respectively, by 1/16 and 1/32. These values are the asymptotic values we can observe by simulation.

Figure 8 displays simulation results for the average information rates with $N_u = 5$ and $N_u = 10$ for continuous-rate, bounded-continuous-rate, and finite-discrete-rate cases. It allows to compare the performance for the different cases (S_1), (S_2), and (S_3). We can see that, due to saturation, we have a significant loss of performance compared to the continuous-rate case. The loss is greater for low noise power. This is due to the strong limitation of the rate, necessary to avoid a bandwidth expansion or some non physically

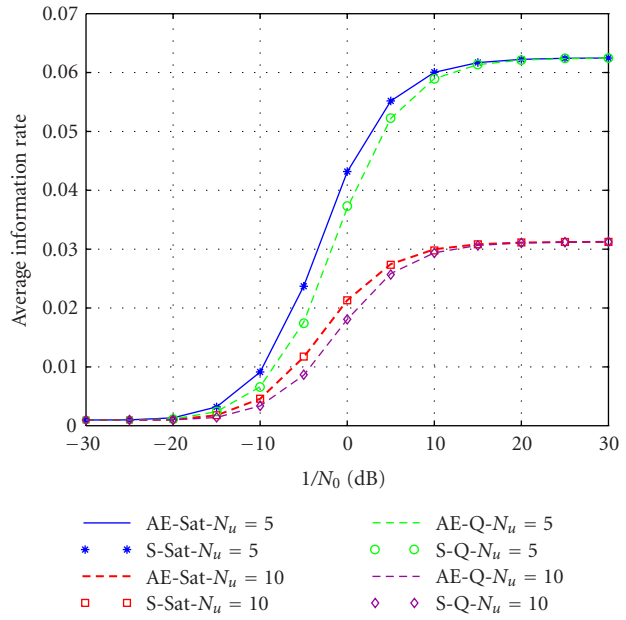

FIGURE 7: Average information rate $\bar{r}$ versus inverse noise $1/N_0$ power in the bounded-continuous-rate (Sat) and the finite-discrete-rate (Q) cases, where (AE) denotes analytic expression and (S) denotes simulation. $N_u = 5, 10$.

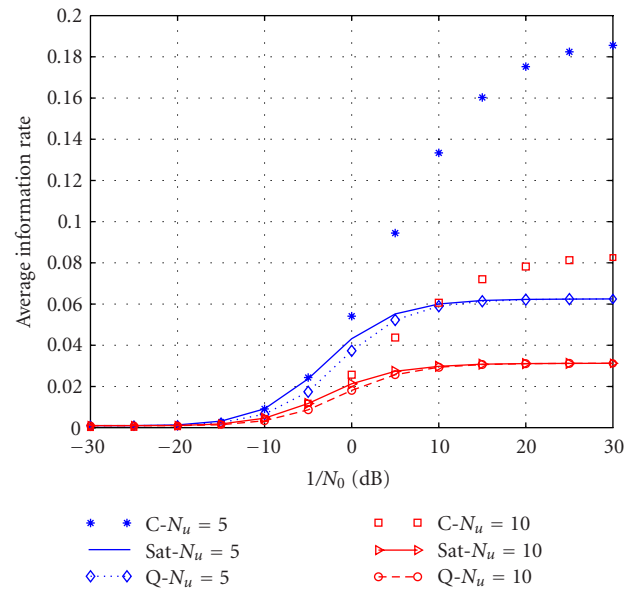

FIGURE 8: Average information rate $\bar{r}$ versus inverse noise power $1/N_0$: simulation results comparison between continuous-rate case (C), bounded-continuous-rate case (Sat), and finite-discrete-rate set case (Q). $N_u = 5, 10$.

reachable rates. The loss due to quantization is less important with respect to the saturated case. Actually, the performance of (S_2) and (S_3) are relatively close. So it seems that the saturation is the constraint which implies the major performance loss.

7. CONCLUSION

In this paper, we have considered the optimization of the transmitters resources in a multiuser time-varying fading environment while guaranteeing a target QoS (CBER) and a connection to any user through the network. We proposed a new link adaptation strategy consisting in the maximization of the minimum user's information rate under the constraint of a required bit energy-to-equivalent noise ratio based on a mean BER for erroneous frames criterion. This is performed through dynamic spreading gain and power control. An easy computational solution to this problem is provided in the continuous-rate case. In more realistic cases with saturation and quantization of the rate's space, we propose suboptimal link adaptation strategies based on a simple saturation of the continuous case or on its quantization. Through simulations, we analyze the influence of finite spreading factor set on the performance of the link adaptation, showing that the main loss is due to saturation.

As shown in the paper, the saturation or quantization of the rates solutions to the continuous case do not give a complete satisfaction due to a performance loss. So, future works will consider the solution to the maximization of the minimum rate, when fully taking into account that the resulting rates can only take their values in a finite set. Moreover, since the system is constrained by the weakest user, we can study alternative or hybrid schemes with classes of users depending on the fading each one encounters (not to be dependent on the weakest user only) and on the kind of service each user demands (different QoS classes modifying the constraint (C_1)).

Another area of interest is the estimation and prediction of the channel parameters by the base station and its feedback to the mobiles. This will involve scheduling and a dynamic study of the side information transmission.

APPENDICES

A. PROOF OF PROPOSITION 1

When

$$\begin{aligned} P_k\alpha_k^2 &= P_{\max}\alpha_1^2, \quad k = 1,\ldots,N_u, \\ r_k &= C\frac{P_{\max}\alpha_1^2}{N_0 + \beta(N_u - 1)P_{\max}\alpha_1^2} = r_0 \quad \forall k, \end{aligned} \tag{A.1}$$

where $C = (E_b/N_e)_t^{-1}$ is the inverse of the desired E_b/N_e. Therefore, $r_{\max-\min}$ satisfying (13) verifies

$$r_{\max-\min} \geq r_0. \tag{A.2}$$

We want to prove that $r_{\max-\min}$ is equal to r_0. We will use a *reductio ad absurdum*. We assume that $r_{\max-\min} > r_0$, therefore all users satisfy $r_k > r_0$, otherwise, there exists one user so that $r_k \leq r_0$. For all $k \neq 1$, let λ_k be defined as

$$P_k\alpha_k^2 = \frac{P_{\max}\alpha_1^2}{\lambda_k}. \tag{A.3}$$

Considering (12), we can also rewrite for all $k' \neq 1$,

$$r_{k'} = \frac{CP_{\max}\alpha_1^2/\lambda_{k'}}{N_0 + \beta P_{\max}\alpha_1^2 \sum_{k\neq 1,k'} 1/\lambda_k + \beta P_1\alpha_1^2}. \tag{A.4}$$

We focus on the subsystem composed by the $N_u - 1$ inequalities defined such that $r_{k'} > r_0$; this is equivalent to

$$\begin{aligned} &\frac{CP_{\max}\alpha_1^2/\lambda_{k'}}{N_0 + \beta P_{\max}\alpha_1^2 \sum_{k\neq 1,k'} 1/\lambda_k + \beta P_1\alpha_1^2} \\ &\quad > \frac{CP_{\max}\alpha_1^2}{N_0 + \beta(N_u-1)P_{\max}\alpha_1^2}, \\ &N_0(1-\lambda_{k'}) + \beta P_{\max}\alpha_1^2\left((N_u-1) - \sum_{k\neq k',1}\frac{\lambda_{k'}}{\lambda_k}\right) \\ &\quad > \beta\lambda_{k'}P_1\alpha_1^2. \end{aligned} \tag{A.5}$$

As for each inequality, the second member is strictly positive, we have also a second subsystem with $N_u - 1$ inequalities by considering the first member strictly positive. We are looking for a solution set $\{\lambda_2, \ldots, \lambda_{N_u}\}$ for these inequalities. If a solution set does not exist, there exists i_0, $r_{i_0} \leq r_0$ and so $r_{\max-\min} \leq r_0$. As $r_{\max-\min} \geq r_0$, this implies that $r_{\max-\min} = r_0$.

If there exists a solution set to this sub-system, let i_0 be the user's index such that, for all user $k \neq 1$, $k \neq i_0$, and $\lambda_{i_0} \geq \lambda_k$. We can consider the following two cases: (1) $\lambda_{i_0} < 1$ and (2) $\lambda_{i_0} \geq 1$. For case (1), for all $k \neq 1$, $\lambda_k < 1$. Thus,

$$r_1 < \frac{CP_1\alpha_1^2}{N_0 + \beta(N_u-1)P_{\max}\alpha_1^2} \leq r_0 \tag{A.6}$$

since $P_1 \leq P_{\max}$. This is in contradiction with the hypothesis that for all k, $r_k > r_0$. For case (2), considering the inequality associated with rate r_{i_0}, we have

$$N_0(1-\lambda_{i_0}) + \beta P_{\max}\alpha_1^2\left((N_u-1) - \sum_{k\neq i_0,1}\frac{\lambda_{i_0}}{\lambda_k}\right) > \beta\lambda_{i_0}P_1\alpha_1^2. \tag{A.7}$$

As $\lambda_{i_0} \geq \lambda_k$,

$$\begin{aligned} &N_0(1-\lambda_{i_0}) + \beta P_{\max}\alpha_1^2 > \beta\lambda_{i_0}P_1\alpha_1^2 \\ &\quad \Longrightarrow P_{\max}\alpha_1^2 > \lambda_{i_0}P_1\alpha_1^2. \end{aligned} \tag{A.8}$$

Finally, we have $P_1 < P_{\max}/\lambda_{i_0}$, which gives us

$$\begin{aligned} r_1 &= \frac{CP_1\alpha_1^2}{N_0 + \beta P_{\max}\alpha_1^2 \sum_{k\neq 1} 1/\lambda_k} \\ &< \frac{CP_{\max}\alpha_1^2/\lambda_{i_0}}{N_0 + \beta(N_u-1)P_{\max}\alpha_1^2/\lambda_{i_0}} \\ &\leq r_0, \end{aligned} \tag{A.9}$$

which is in contradiction with the hypothesis that for all k, $r_k > r_0$.

Finally, we can conclude that $r_{\max-\min} = r_0$.

B. PROOF OF (17)

Using the instantaneous solution to the optimization problem for each frame (15), we can average out over the channel gains described by their pdf (16). The average information rate is given by

$$\begin{aligned} \overline{r} = \mathrm{E}(r) &= \int_0^{+\infty} r_{\max-\min} f_{\alpha_1}(\alpha)d\alpha \\ &= C\int_0^{+\infty} \frac{\alpha^2}{N_0 + \lambda\alpha^2}\frac{2N_u\alpha}{\Omega}e^{-N_u\alpha^2/\Omega}d\alpha, \end{aligned} \tag{B.1}$$

where $C = (E_b/N_e)_t^{-1}P_{\max}$ and $\lambda = \beta(N_u - 1)P_{\max}$.

Let u be defined as $u = N_0 + \lambda\alpha^2$. By variable substitution, it follows that

$$\begin{aligned} \overline{r} &= C\int_0^{+\infty} \frac{\alpha^2}{N_0 + \lambda\alpha^2}\frac{N_u}{\Omega}e^{-N_u\alpha^2/\Omega}2\alpha\, d\alpha \\ &= C\int_{N_0}^{+\infty} \frac{u - N_0}{\lambda u}\frac{N_u}{\Omega}e^{(-N_u/\Omega)((u-N_0)/\lambda)}\frac{du}{\lambda} \\ &= C\frac{N_u}{\Omega\lambda^2}e^{N_uN_0/\Omega\lambda}\int_{N_0}^{+\infty}\frac{u-N_0}{u}e^{-N_uu/\Omega\lambda}du \\ &= C\frac{N_u}{\Omega\lambda^2}e^{N_uN_0/\Omega\lambda}\left(\int_{N_0}^{+\infty}e^{-N_uu/\Omega\lambda}du - N_0\int_{N_0}^{+\infty}\frac{e^{-N_uu/\Omega\lambda}}{u}du\right) \\ &= C\frac{N_u}{\Omega\lambda^2}e^{N_uN_0/\Omega\lambda}(I_1 - I_2). \end{aligned} \tag{B.2}$$

The integral expressions are, respectively, given by

$$\begin{aligned} I_1 &= \int_{N_0}^{+\infty} e^{-N_uu/\Omega\lambda}du \\ &= \frac{\Omega\lambda}{N_u}e^{-N_uN_0/\Omega\lambda} \end{aligned} \tag{B.3}$$

and using variable substitution $v = N_uu/\Omega\lambda$,

$$\begin{aligned} I_2 &= N_0\int_{N_0}^{+\infty} u^{-1}e^{-N_uu/\Omega\lambda}du \\ &= N_0\int_{N_uN_0/\Omega\lambda}^{+\infty}\frac{N_u}{\Omega\lambda}v^{-1}e^{-v}\frac{\Omega\lambda}{N_u}dv \\ &= N_0\int_{N_uN_0/\Omega\lambda}^{+\infty}v^{-1}e^{-v}dv \\ &= N_0\Gamma\left(0, \frac{N_uN_0}{\Omega\lambda}\right), \end{aligned} \tag{B.4}$$

where (19) is the incomplete Gamma function.

C. PROOF OF UPPER BOUND (20)

In the light of (19), we consider the following integral:

$$I = \int_z^{+\infty} v^{-1}e^{-v}dv. \tag{C.1}$$

Considering $V = [z, +\infty)$, since $f(v) = v^{-1} \in L^p(V)$ and $g(v) = e^{-v} \in L^q(V)$ with $1/p + 1/q = 1$ and $p > 1$, $q > 1$, applying Hölder inequality [18], we have

$$I = \int_z^{+\infty} v^{-1} e^{-v} dv \leq \left(\int_z^{+\infty} v^{-p} dv \right)^{1/p} \left(\int_z^{+\infty} e^{-qv} dv \right)^{1/q} \quad \forall p > 1,\ q > 1 \text{ such that } \frac{1}{p} + \frac{1}{q} = 1. \tag{C.2}$$

Moreover,

$$\begin{aligned} I_a &= \left(\int_z^{+\infty} v^{-p} dv \right)^{1/p} = \left(\frac{1}{(p-1)} z^{-p+1} \right)^{1/p} \\ &= (p-1)^{-1/p} z^{(-1+1/p)}, \\ I_b &= \left(\int_z^{+\infty} e^{-qv} dv \right)^{1/q} = \left(\frac{1}{q} e^{-qz} \right)^{1/q} \\ &= q^{-1/q} e^{-z}. \end{aligned} \tag{C.3}$$

Substituting $q = p/(p-1)$, we get

$$I_b = \left(\frac{p}{(p-1)} \right)^{(1/p-1)} e^{-z} = (p-1)^{(1-1/p)} p^{(1/p-1)} e^{-z}. \tag{C.4}$$

Finally, we get the following upper bound for I:

$$I \leq e^{(-z)} z^{(1/p-1)} (p-1)^{(1-2/p)} p^{(1/p-1)} \quad \forall p > 1. \tag{C.5}$$

Applying (C.6) to (19) with $z = (N_u N_0)/(\Omega\lambda)$, we finally have the following expression for I_2:

$$I_2 \leq N_0 e^{(-N_u N_0/\Omega\lambda)} \left(\frac{N_u N_0}{\Omega\lambda} \right)^{(1/p-1)} (p-1)^{(1-2/p)} p^{(1/p-1)} \quad \forall p > 1. \tag{C.6}$$

ACKNOWLEDGMENTS

Part of this work is supported by the French National Network for Telecommunications (RNRT) Project Videophony over IP (VIP). Part of this work has been presented at Fall VTC-03.

REFERENCES

[1] 3GPP, "Physical channels and mapping of transport channels onto physical channels (FDD)," TS 25.211, v. 4.3.0, 2001.
[2] 3GPP, "Multiplexing and channel coding (FDD)," TS 25.212, v. 4.2.0, 2001.
[3] L. Hanzo, P. J. Cherriman, and J. Streit, *Wireless Video Communications: Second to Third Generation and Beyond*, Wiley-IEEE Press, New York, NY, USA, 2001.
[4] S.-J. Oh and K. M. Wasserman, "Dynamic spreading gain control in multiservice CDMA networks," *IEEE Journal on Selected Areas in Communications*, vol. 17, no. 5, pp. 918–927, 1999.
[5] S.-J. Oh, T. L. Olsen, and K. M. Wasserman, "Distributed power control and spreading gain allocation in CDMA data networks," in *Proc. 19th Annual Joint Conference of the IEEE Computer and Communications Societies (INFOCOM '00)*, vol. 2, pp. 379–385, Tel Aviv, Israel, March 2000.
[6] S. A. Jafar and A. Goldsmith, "Adaptive multirate CDMA for uplink throughput maximization," *IEEE Transactions on Wireless Communications*, vol. 2, no. 2, pp. 218–228, 2003.
[7] F. Tang, L. Deneire, M. Engels, and M. Moonen, "A general optimal switching scheme for link adaptation," in *Proc. IEEE Vehicular Technology Conference (VTC '01)*, vol. 3, pp. 1598–1602, Atlantic City, NJ, USA, October 2001.
[8] H. D. Schotten, H. Elders-Bell, and A. Busboom, "Adaptive multi-code CDMA systems for variable data rates," in *Proc. IEEE International Conference on Personal Wireless Communications (ICPWC '97)*, pp. 334–337, Mumbai, India, December 1997.
[9] T. Ottosson and A. Svensson, "Multi-rate performance in DS/CDMA systems," Tech. Rep. 14, Department of Information Theory, Chalmers University of Technology, Göteborg, Sweden, 1995.
[10] T. Ottosson and A. Svensson, "Multi-rate schemes in DS/CDMA systems," in *Proc. IEEE 45th Vehicular Technology Conference (VTC '95)*, vol. 2, pp. 1006–1010, Chicago, Ill, USA, July 1995.
[11] M. Pursley, "Performance evaluation for phase-coded spread-spectrum multiple-access communication—Part I: system analysis," *IEEE Trans. Communications*, vol. 25, no. 8, pp. 795–799, 1977.
[12] G. Caire and E. Viterbo, "Upper bound on the frame error probability of terminated trellis codes," *IEEE Communications Letters*, vol. 2, no. 1, pp. 2–4, 1998.
[13] D. J. Costello Jr. and O. Y. Takeshita, "On the packet error rate of convolutional codes," in *Proc. IEEE Information Theory Workshop and Networking (ITWN '99)*, p. 29, Metsovo, Greece, June 1999.
[14] A. J. Viterbi and J. K. Omura, *Principles of Digital Communication and Coding*, McGraw-Hill, New York, NY, USA, 1979.
[15] J. G. Proakis, *Digital Communications*, McGraw-Hill, New York, NY, USA, 3rd edition, 1995.
[16] A. J. Viterbi, *CDMA: Principles of Spread Spectrum Communication*, Addison-Wesley, Reading, Mass, USA, 1995.
[17] A. Papoulis, *Probability, Random Variables and Stochastic Processes*, McGraw-Hill, New York, NY, USA, 2nd edition, 1984.
[18] P. Henrici, *Applied and Computational Complex Analysis. Volume 3. Discrete Fourier Analysis, Cauchy Integrals, Construction of Conformal Maps, Univalent Functions*, John Wiley & Sons, New York, NY, USA, 1993.

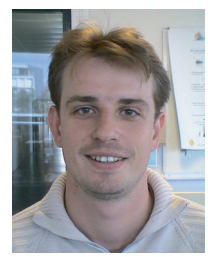

Charly Poulliat received the E.E. degree from the Ecole Nationale Supérieure de l'Electronique et de ses Applications (ENSEA), Cergy-Pontoise, France, in 2001, and the M.S. degree (Diplôme d'Etudes Approfondies) in image and signal processing from the University of Cergy-Pontoise, France, in the same year. He is currently a Ph.D. student at ETIS Laboratory, University of Cergy-Pontoise. His research interests are in physical-layer resource management, iterative decoding techniques, LDPC codes, unequal error protection techniques, and joint source-channel coding/decoding.

Inbar Fijalkow received her Engineering and Ph.D. degrees from Ecole Nationale Supérieure des Télécommunications (ENST), Paris, France, in 1990 and 1993, respectively. In 1993–1994, she was a Research Associate at Cornell University, NY, USA. Since 1994, she is a Member of ETIS Laboratory (UMR 8051), ENSEA/Cergy-Pontoise University/CNRS, Cergy-Pontoise, France. In 1998, she was a Visiting Researcher at the Australian National University (ANU), Canberra, Australia. Her current research interests are in signal processing applied to digital communications; iterative (turbo) processing (in particular, turbo-equalization), analysis of communication systems (including MIMO, OFDM, CDMA, etc.), and optimization of the physical layer resources. She is a Member of the Board of the GDR ISIS, which is the CNRS French national research group on signal, image, and vision processing. She has been an Associate Editor of the IEEE Transactions on Signal Processing from 2000 till 2003.

David Declercq received his Ph.D. in electrical and computer engineering in 1998 from the University of Cergy-Pontoise, France. He is now an Associate Professor at the ETIS Laboratory, Cergy-Pontoise, in the Signal Processing Research Group. He is the Head of the Signal Processing Group since 2003. His research interests are mainly in statistical model estimation and information theory for digital communication. In particular, he is interested in designing good LDPC codes for various types of nonstandard channels (OFDM, multiuser, etc.).

Preliminary call for papers

The 2011 European Signal Processing Conference (EUSIPCO-2011) is the nineteenth in a series of conferences promoted by the European Association for Signal Processing (EURASIP, www.eurasip.org). This year edition will take place in Barcelona, capital city of Catalonia (Spain), and will be jointly organized by the Centre Tecnològic de Telecomunicacions de Catalunya (CTTC) and the Universitat Politècnica de Catalunya (UPC).

EUSIPCO-2011 will focus on key aspects of signal processing theory and applications as listed below. Acceptance of submissions will be based on quality, relevance and originality. Accepted papers will be published in the EUSIPCO proceedings and presented during the conference. Paper submissions, proposals for tutorials and proposals for special sessions are invited in, but not limited to, the following areas of interest.

Areas of Interest

- Audio and electro-acoustics.
- Design, implementation, and applications of signal processing systems.
- Multimedia signal processing and coding.
- Image and multidimensional signal processing.
- Signal detection and estimation.
- Sensor array and multi-channel signal processing.
- Sensor fusion in networked systems.
- Signal processing for communications.
- Medical imaging and image analysis.
- Non-stationary, non-linear and non-Gaussian signal processing.

Submissions

Procedures to submit a paper and proposals for special sessions and tutorials will be detailed at www.eusipco2011.org. Submitted papers must be camera-ready, no more than 5 pages long, and conforming to the standard specified on the EUSIPCO 2011 web site. First authors who are registered students can participate in the best student paper competition.

Important Deadlines:

Proposals for special sessions	15 Dec 2010
Proposals for tutorials	18 Feb 2011
Electronic submission of full papers	**21 Feb 2011**
Notification of acceptance	23 May 2011
Submission of camera-ready papers	6 Jun 2011

Webpage: www.eusipco2011.org

Organizing Committee

Honorary Chair
Miguel A. Lagunas (CTTC)

General Chair
Ana I. Pérez-Neira (UPC)

General Vice-Chair
Carles Antón-Haro (CTTC)

Technical Program Chair
Xavier Mestre (CTTC)

Technical Program Co-Chairs
Javier Hernando (UPC)
Montserrat Pardàs (UPC)

Plenary Talks
Ferran Marqués (UPC)
Yonina Eldar (Technion)

Special Sessions
Ignacio Santamaría (Unversidad de Cantabria)
Mats Bengtsson (KTH)

Finances
Montserrat Nájar (UPC)

Tutorials
Daniel P. Palomar (Hong Kong UST)
Beatrice Pesquet-Popescu (ENST)

Publicity
Stephan Pfletschinger (CTTC)
Mònica Navarro (CTTC)

Publications
Antonio Pascual (UPC)
Carles Fernández (CTTC)

Industrial Liaison & Exhibits
Angeliki Alexiou (University of Piraeus)
Albert Sitjà (CTTC)

International Liaison
Ju Liu (Shandong University-China)
Jinhong Yuan (UNSW-Australia)
Tamas Sziranyi (SZTAKI -Hungary)
Rich Stern (CMU-USA)
Ricardo L. de Queiroz (UNB-Brazil)